Metabolomics: Open Access
ISSN: 2153-0769

Lee et al., Metabolomics 2015, 5:4
DOI: 10.4172/2153-0769.1000152

Short Communication Open Access

Metabolomics Based on UPLC-QTOF/MS Applied for the Discrimination of *Cynanchum wilfordii* and *Cynanchum auriculatum*

Lee Jae-Won[1], Ji Seung-Heon[1], Lee Mi-Kyoung[2], Kim Geum-Soog[1], Ahn Young-Sup[1], Ko Hee-Jung[3], Baek Nam-In[4] and Lee Dae-Young[1*]

[1]*Department of Herbal Crop Research, National Institute of Horticultural and Herbal Science, RDA, Eumseong 27712, Republic of Korea*
[2]*Cancer Preventive Material Development Research Center, College of Oriental Medicine, Kyung Hee University, Seoul 02453, Republic of Korea*
[3]*Waters Corporation, Seoul 07241, Republic of Korea*
[4]*Department of Oriental Medicinal Materials and Processing, Kyung Hee University, Yongin 17104, Republic of Korea*

Abstract

Recently, it has been a big issue to distinguish the dried roots of *Cynanchum wilfordii* and *Cynanchum auriculatum* in Korean herbal medicine market. Although *C. wilfordii* and *C. auriculatum* have similar morphology, the types and quantities of metabolites may differ depending on the species. Thus, in this study, UPLC-QTOF/MS based metabolomics was applied to discriminate the roots of *C. wilfordii* and *C. auriculatum*. In the optimal LC/MS conditions, 64 known metabolites were analyzed in the two species. PCA and PLS-DA of metabolic profile data was able to differentiate between *C. wilfordii* and *C. auriculatum*. Furthermore, OPLS-DA and S-plot were applied to find the potential biomarkers for the discrimination of *C. wilfordii* and *C. auriculatum*. Finally, 4 known and 10 unknown metabolites were determined as the biomarkers, and their repeatability and reliability were also validated. This indicated the metabolite profiling is a robust approach to find discriminating biomarkers of *C. wilfordii* and *C. auriculatum*.

Keywords: *Cynanchum wilfordii*; *Cynanchum auriculatum*; Metabolomics; UPLC-QTOF/MS; PCA; PLS-DA; OPLS-DA

Abbreviations

UPLC-QTOF/MS: Ultra-Performance Liquid Chromatography Coupled with Quadrupole Time-of-Flight/Mass Spectrometry; PCA: Principal Component Analysis; PLS-DA: Partial Least Square-Discriminant Analysis; OPLS-DA: Orthogonal Partial Least Square-Discriminant Analysis

Introduction

The roots of *Cynanchum wilfordii* and *Cynanchum auriculatum* have been widely used as traditional herbal medicines in Eastern Asia. *C. wilfordii* is an ingredient for tonic herbal drugs, and it shows pharmaceutical benefits against tumors, antioxidants, vascular diseases, and diabetes mellitus [1-4]. In China, *C. auriculatum* has been used as a tonic agent having the activities of anti-tumor, gastroprotective, antidepressant, and anti-aging [5-7]. However, in Korea, the human consumption of *C. auriculatum* is still not approved due to its safety concerns. Thus, only the *C. wilfordii* is registered in Korean Herbal Pharmacopoeia [8].

C. wilfordii and *C. auriculatum* belong to the Asclepiadaceae family and appear morphologically similar. In order to discriminate them, it is needed to find the presence of sap and the leaf shapes: *C. auriculatum* has a blade ovate leaf comparing to *C. wilfordii* [9]. However, in the herbal medicine market, they have been handled as cut and dried roots. Due to their similar morphology, it is limited to distinguish the roots of *C. wilfordii* and *C. auriculatum*. Recently in Korea, it has been a critical issue to misuse these two roots in the herbal market and food industry [10]. Thus, it is required to establish a robust tool for the discrimination and quality control of them.

In order to discriminate *C. wilfordii* and *C. auriculatum*, several analytical methods have been previously reported. HPLC–UV method was used to analyze eight marker compounds including conduritol F to discriminate the two species [11]. Phytochemical study was also performed to discover effective chemical markers for their identification [12]. Furthermore, multiplex polymerase chain reaction with specific primers was tried to perform the molecular authentication of similar medicinal plant species [13,14].

Recently, metabolomics based on liquid chromatography (LC) coupled with mass spectrometry (MS) have been used to assess the contents of plant metabolites [15,16]. Plants produce various metabolites in response to developmental, environmental, and stress-induced physiological changes [17-19]. In particular, metabolite profiling by LC/MS is an emerging tool to phenotype and evaluate the quality of plants [20-23]. In this study, we applied the ultra-performance liquid chromatography (UPLC) coupled with quadrupole time-of-flight (QTOF)/MS to analyze various metabolites in the roots of *C. wilfordii* and *C. auriculatum*. Their metabolic profile data was subjected to several multivariate analysis including principal component analysis (PCA), projection to latent structure discriminant analysis (PLS-DA), and orthogonal projections to latent structures discriminant analysis (OPLS-DA) to observe the dissimilarities of metabolites between *C. wilfordii* and *C. auriculatum*. Finally, significant metabolites were selected as the biomarkers to differentiate two species.

Materials and Methods

Herbal medicine samples and reagents

Dried one-year old *Cynanchum wilfordii* (CW) and *Cynanchum auriculatum* (CA) roots were purchased from Yeongju, Gyeongbuk Province, South Korea in 2014. Voucher specimen (NIHHS2014-3) was deposited at the herbarium of the Department of Herbal Crop Research, National Institute of Horticultural and Herbal Science, RDA, Eumseong, Korea. HPLC-grade acetonitrile, methanol, and water were obtained from Merck (Darmstadt, Germany). Formic acid was purchased from Sigma-Aldrich (St. Louis, MO, USA).

***Corresponding author:** DY Lee, Department of Herbal Crop Research, National Institute of Horticultural and Herbal Science, RDA, Eumseong 27712, Republic of Korea, Tel: 82-63-238-6000; E-mail: dylee0809@korea.kr

Received September 28, 2015; **Accepted** October 08, 2015; **Published** October 10, 2015

Citation: Lee JW, Ji SH, Lee MK, Kim GS, Ahn YS, et al. (2015) Metabolomics Based on UPLC-QTOF/MS Applied for the Discrimination of *Cynanchum wilfordii* and *Cynanchum auriculatum*. Metabolomics 5: 152. doi:10.4172/2153-0769.1000152

Copyright: © 2015 Lee JW, et al. This is an open-access article distributed under the terms of the Creative Commons Attribution License, which permits unrestricted use, distribution, and reproduction in any medium, provided the original author and source are credited.

Sample preparation

Each root sample was dried at 35°C in a forced-air-convection-drying oven for three days after washing, and then weighed. The roots were ground (<0.5 mm) using a mixer (Hanil, Seoul, Korea) and thoroughly mixed, after which the subsamples were homogenized further using a Retsch MM400 mixer mill (Retsch GmbH, Haan, Germany) for the analyses. Fine powder was weighed (50 mg), suspended in 10 mL of 70% (v/v) methanol, and ultrasonically extracted for 1 h at 50°C. The extract was filtered and evaporated in a vacuum, and the residue was dissolved in 70% methanol. The solution was filtered through a syringe filter (0.22 μm) and injected directly into the UPLC system.

UPLC-QTOF/MS analysis

UPLC was performed using a Waters ACQUITY H-Class UPLC (Waters Corp.). Chromatographic separations were performed on an ACQUITY BEH C18 column (2.1 mm × 100 mm, 1.7 μm). The column oven was maintained at 40°C and the mobile phases consisted of solvent A [0.1% formic acid (v/v) in water] and solvent B [0.1% formic acid (v/v) in acetonitrile]. The gradient elution program was as follows: 0–2 min, B 10–40%; 2–3.5 min, B 40–45%; 3.5–4.2 min, B 45–55%; 4.2–4.8 min, 55–65%; 4.8–5.2 min, 65–70%; 5.2–10 min, B 70–100%; 10–11 min, B 100–10%; 11–13 min, B 10%. The flow rate was 450 μL/min and 2 μL aliquot of each sample was injected onto the column.

Next, MS analysis was performed using a Waters Xevo G2-S QTOF/MS (Waters Corp.) using an electrospray ionization (ESI) operated in the positive and negative ion mode. The mass spectrometers performed alternative high- and low-energy scans, known as the MS^E acquisition mode. The operating parameters were as follows: cone voltage, 40V; capillary voltage, 3.0 kV; source temperature, 120°C; desolvation temperature, 300°C; cone gas flow, 30 L/h; and desolvation gas flow, 600 L/h. The scan mass range was from 100 and 2,000 *m/z*. The QTOF/MS data was collected in centroid mode, using the lock spray to ensure accuracy and reproducibility. A concentration of 200 pg/mL leucine enkephalin was used as lock mass (*m/z* 556.2766 (ESI+), *m/z* 554.2620 (ESI-)). The lock spray frequency was set at 10 s, and the lock mass data were averaged over 10 scans for correction.

Data processing and multivariate analysis

All MS^E data were collected and processed within UNIFI 1.7.1 and 1.8 Beta (Waters Corp., Milford, USA). Data within UNIFI 1.7.1 and 1.8 Beta is passed through the apex peak detection and alignment processing algorithms. This enables related ion components to be grouped together and analyzed as a single entity. The intensity of each ion was normalized with respect to the total ion count to generate a data matrix that consisted of the retention time, *m/z* value, and the normalized peak area. Charged species, salt adducts, and fragments are all automatically aligned and grouped. The three-dimensional data including peak number (RT-*m/z* pair), sample name, and normalized peak areas were exported to the EZinfo software 3.0.3 (UMETRICS) for multivariate analysis such as unsupervised PCA and the supervised PLS-DA and OPLS-DA. The data were mean-centered and Pareto-scaled prior to PCA, PLS-DA, and OPLS-DA.

Results and Discussion

UPLC-QTOF/MS analysis of various metabolites in the roots of CW and CA

For the effective profiling of various metabolites in the roots of CW and CA, we established a metabolomics platform based on UPLC-QTOF/MS that enables the fast and sensitive analysis with high mass accuracy. Using the optimal UPLC, metabolites extracted using 70% methanol was separated well in 12 min. Both positive and negative ion modes were estimated for the ESI of molecules. As a result, the positive mode showed poor efficiency of ionization (data not shown), and various metabolites of the two roots were successfully analyzed in the negative mode. Thus, only negative mode analysis was performed in this study. Figure 1 represented the base peak intensity (BPI) chromatograms of various metabolites in the two roots.

Next, we constructed the in-house library to identify the metabolites of CW and CA, analyzed by UPLC-QTOF/MS. In practical, it is limited to assign a number of mass spectrums without the database. Previous studies have already reported the presence of various metabolites in CW and CA [6,12,24-26]. Thus, we added the molecular formula of reported compounds into the in-house library. The *m/z* of ions from the raw data of CW and CA was automatically matched to the library compounds. As a result, 69 metabolites were determined with retention time (RT) and mass accuracy (ppm) (Table 1).

PCA and PLS-DA analysis

To visualize the general clustering trends between CW and CA, we applied the multiple pattern recognition methods such as PCA and PLS-DA [27]. First, the constructed method was applied for the metabolite profiling of the extracts obtained from three sample groups including 12 CWs, 12 CAs, and 5 tests (CA:CW mixtures=5:5, 6:4, 7:3, 8:2, 9:1 (w/w)). And then, the processed data was analyzed by PCA and PLS-DA in order to classify the metabolic phenotypes of samples and identify the differentiating metabolites. Unsupervised PCA reduces the dimensionalities of complex datasets and provides an overview of all observations, such as groupings, trends, and outliers [28,29]. In the PCA analysis, the score plot of each sample was shown in Figure 2A. Each point represents an individual sample, and the scatter of samples indicates the similarities or differences of metabolic compositions. Samples having similar metabolite contents are clustered together, whereas those having different metabolites are dispersed. In the PCA score plot, two groups of 12 CWs and 12 CAs were separated well. Furthermore, 5 test samples having different ratio of CW and CA (50%, 60%, 70%, 80%, and 90% CA) were scattered between two groups of CW and CA. However, 5 test samples and CA group were not distinguished clearly. Thus, we also performed the supervised PLS-DA to classify the samples. As a result, the PLS-DA score plot (for the first five components, the goodness of fit of the model (R2Y)=98%, the predictability of the models (Q2)=79%) reflected a clear separation trend among three groups of 12 CWs, 12 CAs, and 5 tests (Figure 2B). Of 5 test samples, the point of 50% CA was positioned almost in the middle of both CW and CA groups. Besides, when the percentage of CA was increased from 50 to 90%, each point was closer to CA groups. This indicated that the metabolic profiles are applicable to not only discriminate CW and CA, but also evaluate the contents ratio of two species.

OPLS-DA analysis

Next, OPLS-DA analysis was performed to find the potential biomarkers for the discrimination of CW and CA. The OPLS-DA score plot showed the clear separation between these two groups (Figure 3A). The scores t [1] (x-axis) and to [1] (y-axis) are the two most important variables in summarizing and separating the data. The separation of CW and CA groups was visible in t [1], and the [1] score values showed the variation within each group. Furthermore, S-plot that shows the covariance p [1] and correlation p (corr) [1] between variables and

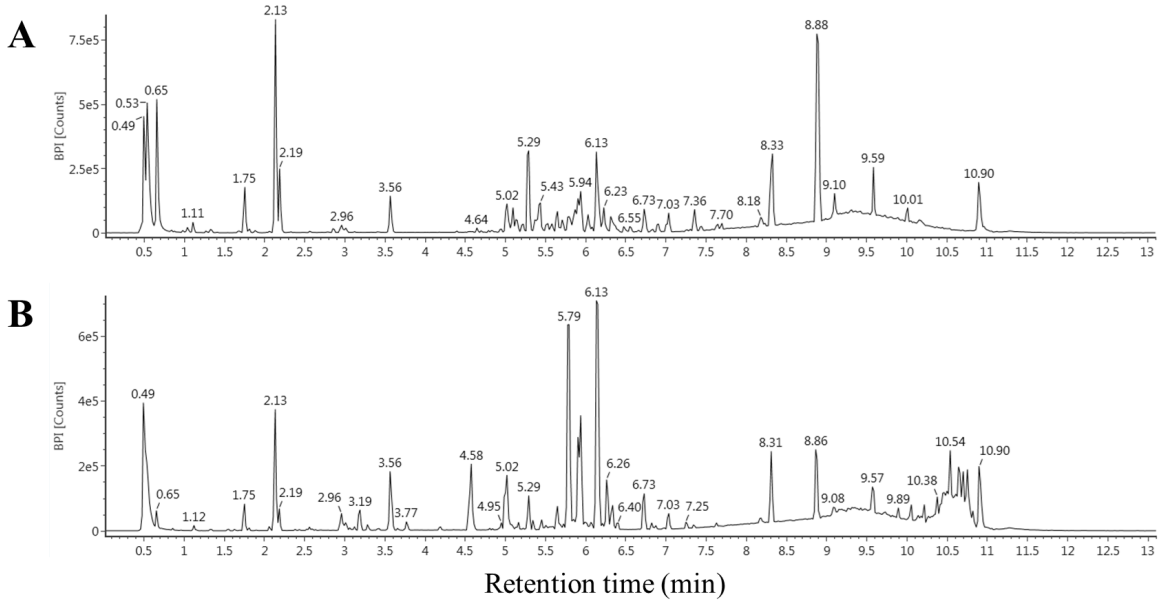

Figure 1: Representative UPLC/QTOF MS-BPI chromatograms of the roots of CW (A) and CA (B) in the negative ion mode.

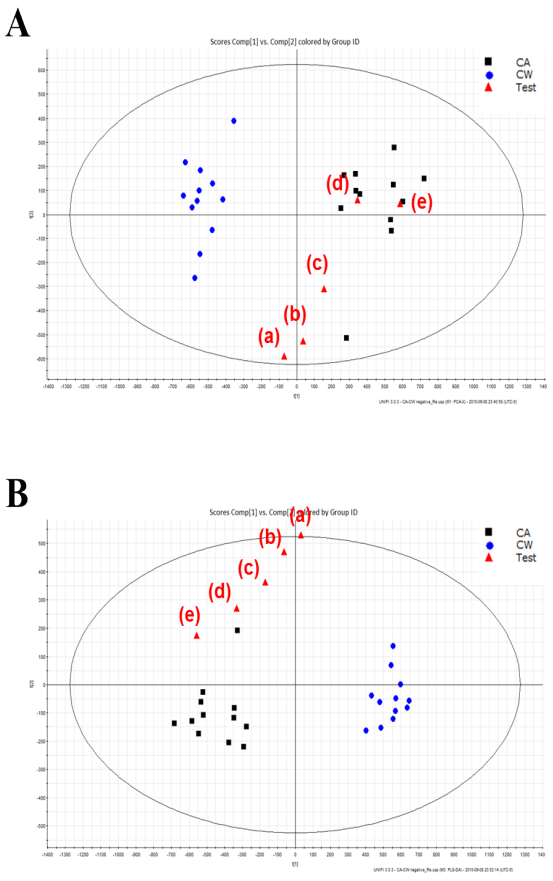

Figure 2: The score plots of PCA (A) and PLS-DA (B) of CA, CW, and Test samples, indicated by boxes, dots, and triangles, respectively. (a) 50% CA; (b) 60% CA; (c) 70% CA; (d) 80% CA; and (e) 90% CA.

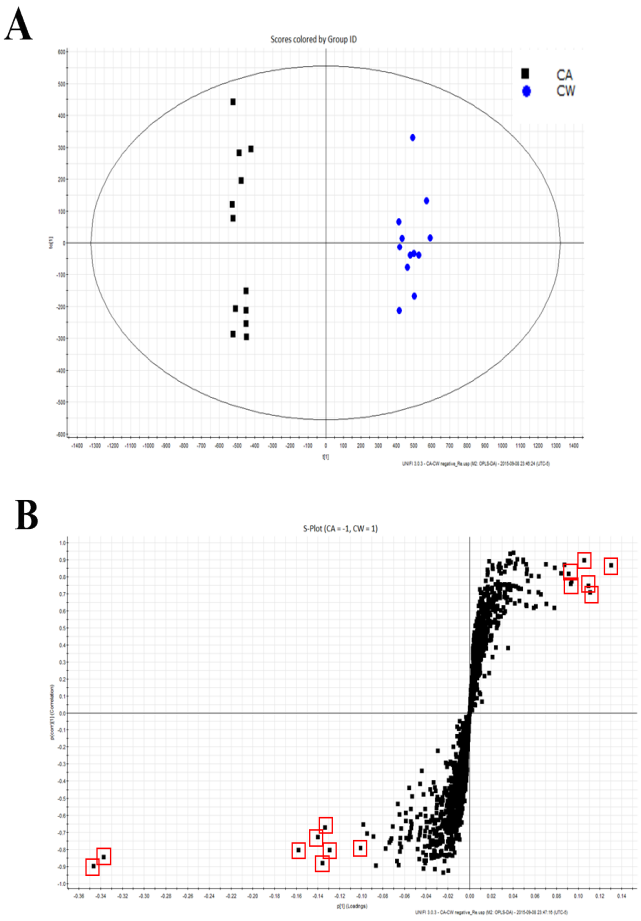

Figure 3: The score plots of OPLS-DA (A) and S-plot (B) of CW and CA samples.

OPLS-DA model was applied to select the critical variables contributing to differentiate CW and CA (Figure 3B). The points in the S-plot represent the *m/z*-RT pairs of molecules. The upper right quadrant of the S-plot shows the components elevated in CW, while the lower left quadrant shows the components elevated in CA. When the point is positioned in the farther along the x-axis and y-axis, the metabolite has the greater contribution and higher reliability to the variance between two groups. In the S-plot, several metabolites were selected as the biomarker candidates. And then, we checked the intensities of each metabolite in whole data to monitor their abundantly difference between CW and CA. As a result, 14 metabolites were selected as the biomarkers. The bar graph represented their altered abundances in CW and CA (Figure 4A). In the analysis of 12 CWs and 12 CAs, 7 and 4 metabolites were almost uniquely detected in CW and CA, respectively. In addition, 3 metabolites were detected in both sides, and showed different abundances. This indicated that the 14 metabolites can be useful biomarkers to discriminate CW and CA.

Identification and validation of selected biomarkers

Based on the in-house library, we tried to identify the selected 14 biomarkers. As a result, 4 ions with *m/z*-RT (1201.6001-4.99, 1435.7114-5.443, 1131.5733-5.78, and 1111.6055-6.13) were identified as Cynauricoside E, Wilfoside C1GG (Cynauricoside C), wilfoside K1N, and wilfoside C1N, respectively. The molecular formula of other 10 ions were also determined by the calculating program, and their RT, mass accuracy, and adducts were listed in Table 2. Next, we performed the validation of 14 biomarkers to find if these biomarkers are repeatable and reliable to discriminate CW and CA. For this purpose, the biomarkers were analyzed in the additional samples of 6 CWs and 6

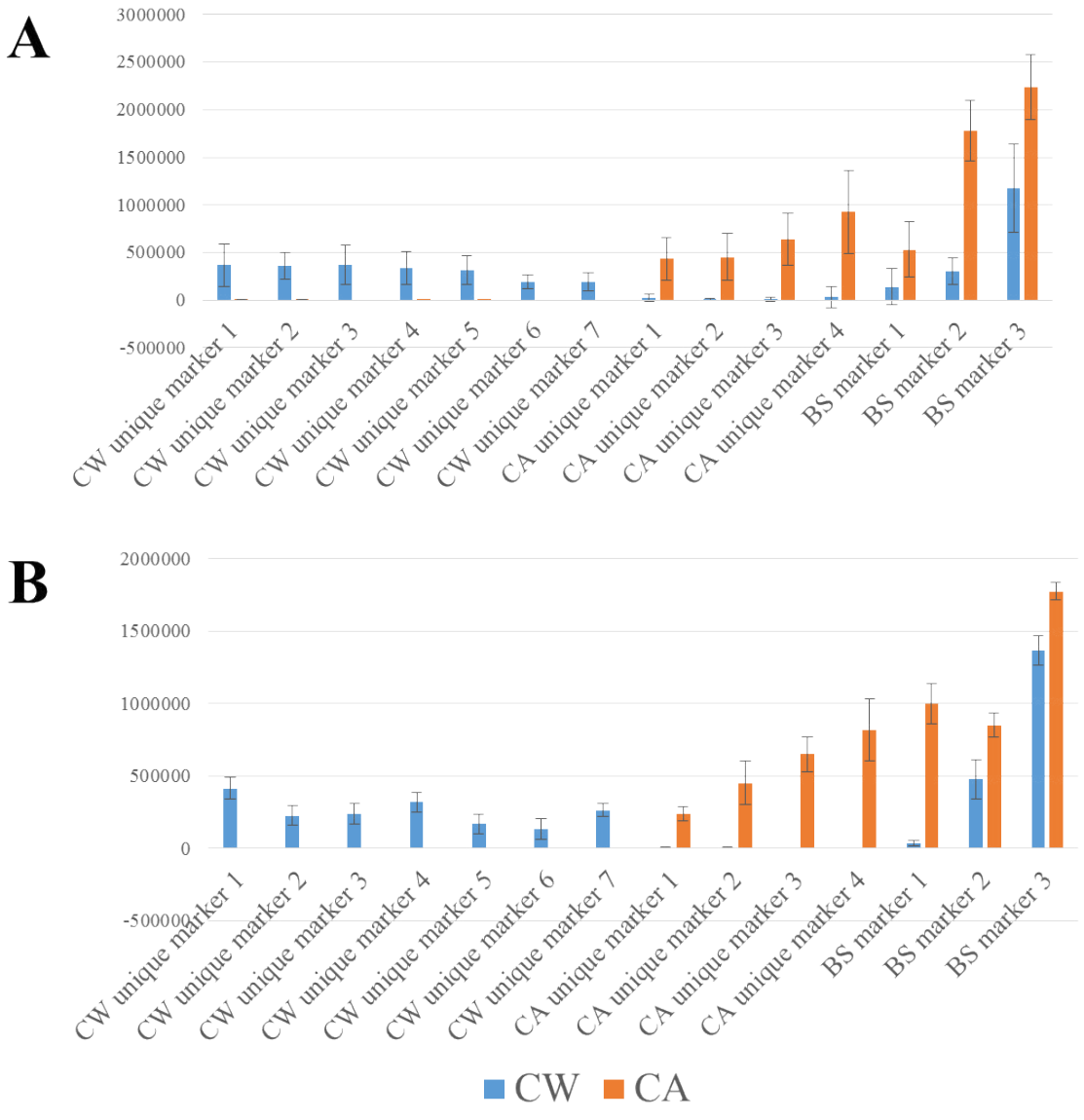

Figure 4: The bar graph of 14 biomarkers altered in CW and CA.

No.	RT (min)	Compound names	Molecular formula	Expected neutral mass (Da)	Observed neutral mass (Da)	QTOF/MS (ESI-) *m/z*	Mass accuracy (ppm)	Adducts
1	0.48	20-O-vanilloyl-kidjoranin	$C_{38}H_{46}O_{10}$	662.3091	662.3075	707.3057	-2.3	+HCOO
2	0.48	Geniposide	$C_{17}H_{24}O_{10}$	388.1369	388.1368	433.135	-0.36	+HCOO
3	0.48	Qingyangshengenin	$C_{28}H_{36}O_{8}$	500.241	500.24	545.2382	-1.79	+HCOO
4	0.53	Conduritol F	$C_{6}H_{10}O_{4}$	146.0579	146.0583	191.0565	2.23	+HCOO
5	0.68	Succinic acid	$C_{4}H_{6}O_{4}$	118.0266	118.027	117.02	1.18	-H
6	0.84	Cynanoneside B	$C_{14}H_{18}O_{8}$	314.1002	314.1002	313.0929	-0.03	-H
7	1.76	*p*-hydroxyacetophenone	$C_{8}H_{8}O_{2}$	136.0524	136.0524	135.0452	0	-H
8	1.82	Acetovanillone	$C_{9}H_{10}O_{3}$	166.063	166.0629	165.0556	-0.44	-H
9	2.03	Resacetophenone	$C_{8}H_{8}O_{3}$	152.0473	152.0472	151.0399	-0.98	-H
10	2.14	Cynandione A	$C_{16}H_{14}O_{6}$	302.079	302.079	301.0718	-0.03	-H
11	2.14	Scopoletin	$C_{10}H_{8}O_{4}$	192.0423	192.0409	191.0336	-7.35	-H
12	2.6	Penupogenin	$C_{30}H_{40}O_{7}$	512.2774	512.2773	511.27	-0.25	-H
13	2.81	Cynanchone A	$C_{17}H_{16}O_{6}$	316.0947	316.0947	315.0874	0.03	-H
14	2.83	Cynauricoside H	$C_{47}H_{76}O_{18}$	928.5032	928.5058	973.504	2.66	+HCOO
15	3.39	Cynauricoside F	$C_{54}H_{88}O_{21}$	1072.5818	1072.5823	1117.5805	0.45	+HCOO
16	4.42	Kidjoranin	$C_{30}H_{38}O_{7}$	510.2618	510.2664	555.2646	8.38	+HCOO
17	4.68	Cyanoauriculoside A	$C_{72}H_{110}O_{30}$	1454.7082	1454.7078	1499.706	-0.27	+HCOO
18	4.78	Caudatin	$C_{28}H_{42}O_{7}$	490.2931	490.2932	535.2914	0.25	+HCOO
19	4.81	Cynanauriculoside E	$C_{60}H_{98}O_{26}$	1232.619	1232.619	1277.6172	-0.01	+HCOO
20	4.83	Wilfoside K 1GG	$C_{70}H_{106}O_{29}$	1410.682	1410.682	1455.6802	0	+HCOO
21	4.93	Otophylloside L	$C_{61}H_{98}O_{26}$	1246.6346	1246.6328	1291.631	-1.42	+HCOO
22	4.94	Caudatin 3-O-β-D-digitoxopyranoside	$C_{34}H_{52}O_{10}$	620.356	620.3561	665.3543	0.12	+HCOO
23	4.94	Cynanauriculoside D	$C_{61}H_{92}O_{27}$	1256.5826	1256.5828	1301.581	0.18	+HCOO
24	4.99	Cynauricoside E	$C_{58}H_{92}O_{23}$	1156.6029	1156.6019	1201.6001	-0.83	+HCOO
25	5.08	Wilfoside E	$C_{62}H_{94}O_{23}$	1206.6186	1206.6175	1205.6102	-0.92	-H
26	5.43	Wilfoside C 1GG	$C_{68}H_{110}O_{29}$	1390.7133	1390.7132	1435.7114	-0.06	+HCOO
27	5.12	Deacylmetaplexigenin	$C_{21}H_{32}O_{6}$	380.2199	380.2194	379.2121	-1.23	-H
28	5.21	Wilfoside A	$C_{50}H_{67}NO_{14}$	905.4562	905.4563	950.4545	0.17	+HCOO
29	5.3	Cynauriculoside A	$C_{70}H_{108}O_{24}$	1332.7231	1332.7209	1377.7191	-1.59	+HCOO
30	5.34	Cynauricoside I	$C_{49}H_{78}O_{19}$	970.5137	970.5143	969.507	0.57	-H
31	5.4	Cynauricoside C	$C_{65}H_{96}O_{23}$	1244.6342	1244.6347	1289.6329	0.36	+HCOO
32	5.45	Wilfoside G	$C_{60}H_{88}O_{20}$	1128.5869	1128.587	1173.5852	0.1	+HCOO
33	5.46	Auriculoside B	$C_{61}H_{98}O_{24}$	1214.6448	1214.6455	1259.6437	0.54	+HCOO
34	5.46	Cynandione D	$C_{32}H_{24}O_{10}$	568.1369	568.1372	567.1299	0.44	-H
35	5.53	Wilfoside D1N	$C_{56}H_{84}O_{19}$	1060.5607	1060.5605	1105.5587	-0.19	+HCOO
36	5.57	Caudatin 3-O-β-D-cymaropyranoside	$C_{35}H_{54}O_{10}$	634.3717	634.3719	679.3701	0.36	+HCOO
37	5.57	Cynanauriculoside II	$C_{77}H_{118}O_{30}$	1522.7708	1522.7725	1567.7707	1.11	+HCOO
38	5.59	Wilfoside H	$C_{53}H_{76}O_{17}$	984.5083	984.5082	1029.5064	-0.07	+HCOO
39	5.6	Cyanoauriculoside B	$C_{66}H_{100}O_{25}$	1292.6554	1292.6542	1291.6469	-0.89	-H
40	5.65	Cynauricoside A	$C_{51}H_{74}O_{16}$	942.4977	942.4977	987.4959	0.05	+HCOO
41	5.68	Cynauricoside B	$C_{63}H_{94}O_{22}$	1202.6237	1202.624	1247.6222	0.25	+HCOO
42	5.69	Cynanauriculoside F	$C_{60}H_{90}O_{20}$	1130.6025	1130.6018	1175.6	-0.62	+HCOO
43	5.71	Wilfoside B	$C_{48}H_{70}O_{14}$	870.4766	870.4804	915.4786	4.24	+HCOO
44	5.78	Wilfoside K1N	$C_{58}H_{86}O_{19}$	1086.5763	1086.5751	1131.5733	-1.06	+HCOO
45	5.88	Wilfoside D	$C_{55}H_{82}O_{20}$	1062.5399	1062.5396	1107.5379	-0.27	+HCOO
46	5.9	Cyanoauriculoside C	$C_{62}H_{94}O_{22}$	1190.6237	1190.623	1189.6157	-0.57	-H
47	5.98	Cynauricoside G	$C_{56}H_{90}O_{22}$	1114.5924	1114.5928	1113.5855	0.34	-H
48	5.99	Wilfoside C1G	$C_{62}H_{100}O_{24}$	1228.6605	1228.6604	1227.6531	-0.08	-H
49	6.04	Kidjoranin 3-O-β-D-digitoxopyranoside	$C_{36}H_{48}O_{10}$	640.3247	640.3246	639.3173	-0.21	-H
50	6.05	Cynanauriculoside I	$C_{76}H_{116}O_{30}$	1508.7551	1508.7555	1553.7537	0.2	+HCOO
51	6.14	Wilfoside C1N	$C_{56}H_{90}O_{19}$	1066.6076	1066.6073	1111.6055	-0.34	+HCOO
52	6.64	Wilfoside F	$C_{62}H_{100}O_{22}$	1196.6706	1196.671	1241.6692	0.33	+HCOO
53	7.17	Daucosterol	$C_{35}H_{60}O_{6}$	576.439	576.4387	621.4369	-0.41	+HCOO
54	7.58	9,12,15-Octadecatrienoic acid	$C_{18}H_{30}O_{2}$	278.2246	278.2245	277.2172	-0.23	-H
55	8.32	Metaplexigenin	$C_{23}H_{34}O_{7}$	422.2305	422.2308	421.2235	0.83	-H
56	8.33	Linoleic acid	$C_{18}H_{32}O_{2}$	280.2402	280.2402	279.233	-0.01	-H

57	9.09	3-O-methyl-caudatin	$C_{29}H_{44}O_7$	504.3087	504.3078	549.306	-1.72	+HCOO
58	9.11	Hexadecanoic acid	$C_{16}H_{32}O_2$	256.2402	256.2402	255.233	-0.01	-H
59	9.19	Oleic acid	$C_{18}H_{34}O_2$	282.2559	282.2559	281.2486	0.04	-H
60	9.6	Sarcostin	$C_{21}H_{34}O_6$	382.2355	382.2346	381.2274	-2.37	-H
61	9.89	Gagaminine	$C_{36}H_{43}NO_8$	617.2989	617.2996	616.2923	1.22	-H
62	10.17	Octadecanoic acid	$C_{18}H_{36}O_2$	284.2715	284.2716	283.2643	0.15	-H
63	10.49	20-O-salicyl-kidjoranin	$C_{37}H_{44}O_9$	632.2985	632.299	631.2917	0.71	-H
64	10.93	Wilfoside C	$C_{48}H_{70}O_{17}$	918.4613	918.4611	917.4538	-0.21	-H

Table 1: The *in-house* library of various metabolites in CW and CA.

No.	Biomarkers		RT (min)	Molecular formula	Expected neutral mass (Da)	Observed neutral mass (Da)	QTOF/MS (ESI-) *m/z*	Mass accuracy (ppm)	Adducts
1	CW unique marker 1	Wilfoside C 1GG	5.43	$C_{68}H_{110}O_{29}$	1390.7133	1390.7132	1435.7114	-0.06	+HCOO
2	CW unique marker 2	Unknown	6.23	$C_{76}H_{124}O_{30}$	1516.8177	1516.8189	1561.8158	0.79	+HCOO
3	CW unique marker 3	Unknown	6.17	$C_{71}H_{108}O_{25}$	1360.718	1360.7202	1405.7179	1.62	+HCOO
4	CW unique marker 4	Unknown	5.89	$C_{69}H_{112}O_{27}$	1372.7391	1372.7417	1417.732	1.87	+HCOO
5	CW unique marker 5	Unknown	6.31	$C_{77}H_{118}O_{28}$	1490.781	1490.7831	1535.7826	1.45	+HCOO
6	CW unique marker 6	Unknown	6.905	$C_{78}H_{120}O_{28}$	1504.7966	1504.7958	1549.7952	-0.55	+HCOO
7	CW unique marker 7	Unknown	7.44	$C_{70}H_{114}O_{25}$	1354.7649	1354.7643	1399.7622	1.25	+HCOO
8	CA unique marker 1	Unknown	6.26	$C_{72}H_{110}O_{25}$	1374.7336	1374.7334	1419.7315	1.06	+HCOO
9	CA unique marker 2	Unknown	3.19	$C_{49}H_{80}O_{18}$	956.5345	956.5343	1001.5321	-0.13	+HCOO
10	CA unique marker 3	Cynauricoside E	4.99	$C_{58}H_{92}O_{23}$	1156.6029	1156.6019	1201.6001	-0.83	+HCOO
11	CA unique marker 4	Unknown	4.58	$C_{51}H_{82}O_{19}$	998.545	998.5433	1043.5408	-0.86	+HCOO
12	*BS marker 1	Unknown	6.71	$C_{70}H_{114}O_{25}$	1354.7649	1354.7675	1399.7622	1.25	+HCOO
13	BS marker 2	Wilfoside K1N	5.78	$C_{58}H_{86}O_{19}$	1086.5763	1086.5751	1131.5733	-1.06	+HCOO
14	BS marker 3	Wilfoside C1N	6.14	$C_{56}H_{90}O_{19}$	1066.6076	1066.6073	1111.6055	-0.34	+HCOO

Table 2: The list of biomarkers to discriminate CW and CA (*Both sides).

CAs, and the bar graph of 14 biomarkers validation was represented in Figure 4B. As a result, the additional analysis of 14 biomarkers showed the almost similar results with previous analysis. Although the fold change of Biomarker 12, 13, and 14 was altered, CA showed the higher abundance of them.

Conclusion

In this study, metabolomics approach based on UPLC-QTOF/MS provided the effective discrimination of CW and CA. By the optimal LC/MS conditions, the fast and sensitive analysis of 64 metabolites in CW and CA were successfully performed. In the PCA and PLS-DA, not only two groups of CW and CA but also their mixture samples having different ratio were differentiated well. Next, OPLS-DA and S-plot were also applied for the selection of biomarkers to discriminate CW and CA. Based on the quantification of 14 selected molecules, we determined 7 CW unique, 4 CA unique, and 3 both sides biomarkers. Our results indicated the UPLC-QTOF/MS based metabolite profiling is promising to differentiate CW and CA that have morphological similarity. Hence, this work is of great importance to prevent the misuse of CW and CA especially in the Korean herbal market.

Acknowledgements

This work was carried out with the support of "Cooperative Research Program for Agriculture Science & Technology Development (Project No. PJ01136203)" Rural Development Administration, Republic of Korea.

References

1. Brown PD, Tokuhisa JG, Reichelt M, Gershenzon J (2003) Variation of glucosinolate accumulation among different organs and developmental stages of Arabidopsis thaliana. Phytochem 62: 471-481.
2. Choi DH, Lee YJ, Kim JS, Kang DG, Lee HS, et al. (2012a) *Cynanchum wilfordii* ameliorates hypertension and endothelial dysfunction in rats fed with high fat/cholesterol diets. Immunopharmacol Immunotoxicol 34: 4-11.
3. Choi DH, Lee YJ, Oh HC, Cui YL, Kim JS, et al. (2012b) Improved Endothelial Dysfunction by *Cynanchum wilfordii* in Apolipoprotein $E^{-/-}$ Mice Fed a High Fat/Cholesterol Diet. J Med Food 15: 169-179.
4. Gunes A, Inal A (2007) Salicylic acid induced changes on some physiological parameters symptomatic for oxidative stress and mineral nutrition in maize (*Zea mays* L.) grown under salinity. J Plant Physiol 164: 728-736.
5. Gu XJ, Yao N, Qian SH, Li YB, Li P, et al. (2009) Four new C21 steroidal glycosides from the roots of *Cynanchum auriculatum*. Hel Chim Acta 92: 88-97.
6. Jiang YF, Choi HG, Li Y, Park YM, Lee JH, et al. (2011) Chemical Constituents of *Cynanchum wilfordii* and the Chemotaxonomy of Two Species of the Family Asclepiadacease, *C. wilfordii* and *C. auriculatum*. Arch Pharm Res 34: 2021-2027.
7. KFDA (2008) The 9th Korean Herbal Pharmacopoeia.
8. Kim MS, Baek JH, Park JA, Hwang BY, Kim SE, et al. (2005) Wilfoside K1N isolated from *Cynanchum wilfordii* inhibits angiogenesis and tumor cell invasion. Int J Oncol 26: 1533-1539.
9. Choi KA (2015) Fake medicine hits retail investors hard. The Korea Times.
10. Lee DW, Kim CH, Le DU (2001) Effect of Culture Conditions on the Biosynthesis of Gagaminine, a Potent Antioxidant from the Roots of *Cynanchum wilfordii*. Bio Pharm Bull 24: 1451-1453.
11. Lee DY, Kim JK, Shrestha S, Seo KH, Lee YH, et al. (2013) Quality Evaluation of Panax ginseng Roots Using a Rapid Resolution LC-QTOF/MS-Based Metabolomics Approach. Molecules 18: 14849-14861.
12. Li Y, Piao D, Zhang H, Woo MH, Lee JH, et al. (2013) Quality assessment and discrimination of the roots of *Cynanchum auriculatum* and *Cynanchum wilfordii* by HPLC–UV analysis. Arch Pharm Res 36: 335-344.
13. Liede S, Tauber A (2002) Circumscriptionof the Genus Cynanchum (Apocynaceae-Asclepiadoideae). Am Soc Plant Taxonomists 27: 789-800.
14. Liu JH, Kitashiba H, Wang J, Ban Y, Moriguchi T, et al. (2007) Polyamines and their ability to provide environmental stress tolerance to plants. Plant Biotechnol 24: 117-126.

15. Moon BC, Choo BK, Cheon MS, Yoon T, Ji Y, et al. (2010) Rapid molecular authentication of three medicinal plant *Cynanchum wilfordii, Cynanchum auriculatum,* and *Polygonum multiflorum (Fallopia multiflorum)*, by the development of RAPD-derived SCAR markers and multiplex-PCR. Plant Biotechnol Rep 4: 1-7.

16. Qi LW, Gu XJ, Li P, Liang Y, Hao H, et al. (2009). Structural characterization of pregnane glycosides from *Cynanchum auriculatum* by liquid chromatography on a hybrid ion trap time-of-flight mass spectrometer. Rapid Commun Mass Spectrom 23: 2151-2160.

17. Ryuk JA, Lee HW, Ju YS, Ko BS (2014) Monitoring and Identification of *Cynanchum wilfordii* and *Cynanchum auriculatum* by Using Molecular Markers and Real-Time Polymerase Chain Reaction. J Korean Soc App BI 57: 245-251.

18. Schauer N, Fernie AR (2006) Plant metabolomics: towards biological function and mechanism. Trends Plant Sci 11: 508-516.

19. Shan L, Liu RH, Shen YH, Zhang WD, Zhang C, et al. (2006) Gastroprotective effect of a traditional Chinese herbal drug “Baishouwu” on experimental gastric lesions in rats. J Ethnopharmacol 107: 389-394.

20. Steinmann D, Ganzera M (2011) Recent advances on HPLC/MS in medicinal plant analysis. J Pharm Biomed Anal 55: 744-757.

21. Sultana T, Stecher G, Mayer R, Trojer L, Qureshi MN, et al. (2008) Quality Assessment and Quantitative Analysis of Flavonoids from Tea Samples of Different Origins by HPLC-DAD-ESI-MS. J Agric Food Chem 56: 3444-3453.

22. Sumner LW, Mendes P, Dixon RA (2003) Plant metabolomics: large-scale phytochemistry in the functional genomics era. Phytochem 62: 817-836.

23. Sun L, Li J, Zhou K, Zhang M, Yang J, et al. (2013) Metabolomic analysis reveals metabolic disturbance in the cortex and hippocampus of subchronic MK-801 treated rats. PLoS ONE 8: e60598.

24. Trygg J, Holmes E, Lundstedt T (2007) Chemometrics in metabonomics. J Proteome Res 6: 469-479.

25. De Vos RC, Moco S, Lommen A, Keurentjes JJ, Bino RJ, et al. (2007) Untargeted large-scale plant metabolomics using liquid chromatography coupled to mass spectrometry. Nat Protoc 2: 778-791.

26. Wang YQ, Zhang SJ, Lu H, Yang B, Ye LF, et al. (2013) A C21-Steroidal Glycoside Isolated from the Roots of *Cynanchum auriculatum* Induces Cell Cycle Arrest and Apoptosis in Human Gastric Cancer SGC-7901 Cells. Evid Based Complement Alternat Med 1-7.

27. Wang M, Yang X, Wang F, Li R, Ning H, et al. (2013b) Calcium-deficiency assessment and biomarker identification by an integrated urinary metabolomics analysis. BMC Medicine 11:86.

28. Xiang, WJ, Ma L (2009) C21 steroidal glycosides from *Cynanchum wilfordii*. Hel Chim Acta 92: 2659-2674.

29. Yang QX, Ge YC (2011) Cynanauriculoside C–E, three new antidepressant pregnane glycosides from *Cynanchum auriculatum*. Phytochem Lett 4: 170-175.